

A Novel Phospholipase D2-Grb2-WASp Heterotrimer Regulates Leukocyte Phagocytosis in a Two-Step Mechanism[∇]

Samuel Kantonen,¹ Nathaniel Hatton,¹ Madhu Mahankali,¹ Karen M. Henkels,¹ Haein Park,² Dianne Cox,² and Julian Gomez-Cambroner^{1*}

Department of Biochemistry and Molecular Biology, Wright State University School of Medicine, Dayton, Ohio 45435,¹ and Department of Anatomy, Structural Biology and Developmental and Molecular Biology, Albert Einstein College of Medicine, Jack and Pearl Resnick Campus, Bronx, New York 10461²

Received 22 May 2011/Returned for modification 21 June 2011/Accepted 8 September 2011

Phagocytosis is a primary innate response of both macrophages and neutrophils involving the formation of filamentous actin (F-actin)-rich protrusions that are extended around opsonized pathogens to form a phagocytic cup, resulting in their subsequent internalization. The molecular mechanism for this is still not completely understood. We now show for the first time that phospholipase D2 (PLD2) binds to growth factor receptor-bound protein 2 (Grb2) and to the Wiskott-Aldrich syndrome protein (WASp) to form a heterotrimer complex, PLD2-Grb2-WASp, and present the mechanism of interaction. Grb2 binds to the Y169/Y179 residues of PLD2 using its only SH2 domain, and it interacts with the poly-proline region of WASp using its two SH3 domains. The PLD2-Grb2-WASp heterotrimer can be visualized in early phagocytic cups of macrophages ingesting opsonized red blood cells, where it associates with polymerized actin. Cup colocalization and phagocytosis are disrupted with mutants that alter binding at either of the two proteins or by silencing Grb2 with RNA interference (RNAi). WASp association to PLD2-K758R, a lipase-inactive mutant, still occurs, albeit at lower levels, indicating that PLD2 plays a second role in phagocytosis, which is the production of phosphatidic acid (PA) and activation of phosphatidylinositol 5-kinase (PI5K) with subsequent synthesis of phosphatidylinositol 4,5-bisphosphate (PIP₂). The latter can be blocked with RNAi, which negates phagocytosis. Lastly, a constitutively “open” active form of WASp (WASp-L270P) brings phagocytosis to its maximum level, which can be mimicked with WASp-WT plus PLD2 or plus PA. Since neither a protein-protein disruption nor lack of PLD activity completely negates cup formation or phagocytosis, we posit a two-step mechanism: PLD2 anchors WASp at the phagocytic cup through Grb2 following protein-protein interactions and also activates it, making key lipids available locally. The heterotrimer PLD2-Grb2-WASp then enables actin nucleation at the phagocytic cup and phagocytosis, which are at the center of the innate immune system function.

Phagocytosis is a primary innate response of both macrophages and neutrophils, which involves Fcγ receptors for opsonized pathogens or foreign particles. Activation of these receptors results in filamentous actin (F-actin)-rich protrusions that are extended around the bound particle to form a phagocytic cup, resulting in its subsequent internalization. Wiskott-Aldrich syndrome protein (WASp) is a key regulator in the formation of these cups, and in particular, the C-terminal activity of the verprolin-cofilin-acidic (VCA) region is essential (18, 30, 31). WASp is an essential protein in hematopoietic cells, which binds to cofilin and the Arp2/3 complex in order to disassemble and then repolymerize actin monomers (G-actin) into F-actin, respectively, while N-WASp is present in all cells of the body (21). The crucial process of actin polymerization is the basis on which cells change their shape or move through their environment. WASp has been shown to be activated by the small Rho family GTPase Cdc42 through its GTPase binding domain (GBD) but also by phosphatidylinositol 4,5-bisphosphate (PIP₂) through WASp's basic region (9, 11, 27, 32). Both of these regions are upstream from the conserved VCA

region at the end of the carboxy terminus, which is the essential catalytic region required for WASp activity (14, 19, 23). While the role of Cdc42 in WASp activation in response to receptor activation has been studied with purified proteins, the regulation of WASp by other means within the actual cell and its localization to the cup is not entirely understood.

Phospholipase D2 (PLD2) is a membrane-associated lipase that catalyzes the breakdown of phosphatidylcholine into phosphatidic acid (PA) and choline. PA has been shown to be an important signaling molecule involved in many cellular processes, such as membrane trafficking, cell invasion, cell growth, and anti-apoptosis (2). Growth factor receptor-bound protein 2 (Grb2) has been shown to interact with PLD2 via its three regions: two Src homology 3 (SH3) domains (which bind poly-proline motifs) and one Src homology 2 (SH2) domain (which binds certain phosphorylated tyrosine motifs) (5, 7).

Based on the distinct ability of PLD2 to regulate PIP₂ and its presence at the plasma membrane, we have hypothesized that a WASp-PLD2 interaction would allow for simultaneous activation of WASp and recruitment of WASp to the membrane where phagocytic cups may begin to form. We show here that an intermediate protein is required, Grb2. Through Grb2, WASp is localized and anchored to the membrane by PLD2, which then drives the activation of WASp through lipids and the subsequent formation of phagocytic cups. We posit that the presence of this new heterotrimer, PLD2-Grb2-WASp, is necessary for leukocyte phagocytosis.

* Corresponding author. Mailing address: Dept. of Biochemistry and Molecular Biology, Wright State University School of Medicine, 3640 Colonel Glenn Highway, Dayton, OH 45435. Phone: (937) 775-3601. Fax: (937) 775-3730. E-mail: julian.cambroner@wright.edu.

[∇] Published ahead of print on 19 September 2011.

MATERIALS AND METHODS

Cultured cells. RAW/LR5 cells were cultured in reduced bicarbonate DMEM plus 10% fetal calf serum (FCS). COS-7 cells were cultured in Dulbecco's modified Eagle's medium (DMEM) plus 10% newborn calf serum (NCS). The plasmids used in this experiment were as follows: pcDNA3.1-mycPLD2-WT, pcDNA3.1-mycPLD2-K758R, pcDNA3.1-mycPLD2-Y169F, pcDNA3.1-mycPLD2-Y179F, pcDNA3.1-mycPLD2-Y169F/Y179F, pcDNA3.1-XGrb2, pcDNA3.1-XGrb2-R86K, pcDNA3.1-XGrb2-P49/206L, pEGFP-C1-Grb2, mCit-C1-PLD2-WT, pU627-shGrb2, pEGFP-C1-WASp, pEF-BOS-mycWASp-L270P, and pEF-BOS-mycWASp-L270P/Y291F. When cultured cells reached a confluence of ~60%, they were transfected with the plasmid of interest.

Cell transfection. Transfections were done using 5 μ l Lipofectamine (Invitrogen, Carlsbad, CA) and 5 μ l Plus reagent (Invitrogen) in Opti-MEM medium (Invitrogen) previously mixed in sterile glass test tubes. COS-7 cells were transfected for 3 h and were washed and refed with prewarmed complete medium. After 36 h, cells were harvested for their respective experiment. For the RAW/LR5 cells, cells were transfected using the Superfect reagent (Qiagen, Valencia, CA). Superfect was used in a ratio of 5:1 μ l/ μ g DNA per transfection. The DNA and Superfect were mixed in posttransfection medium (without antibiotics), applied to the cells, transfected for 36 h, and then harvested for their respective experiment.

Coimmunoprecipitation. After transfection, cells were harvested and lysed with Special lysis buffer (5 mM HEPES, pH 7.8, 100 μ M sodium orthovanadate, and 0.1% Triton X-100). The lysates were sonicated and treated with 1 μ l monoclonal antibody for the respective protein and 10 μ l agarose beads (Millipore, Billerica, MA) and incubated at 4°C for 4 h. After incubation, the immunoprecipitates were washed with LiCl wash buffer (2.1% LiCl, 1.6% Tris-HCl, pH 7.4) and NaCl wash buffer (0.6% NaCl, 0.16% Tris-HCl, 0.03% EDTA, pH 7.4), respectively, and sedimented at 12,000 \times g for 1 min. The resulting pellets were then analyzed using SDS-PAGE and Western blot (WB) analyses.

Gene silencing. Grb2 expression in RAW/LR5 cells was downregulated using the following two different methods: small interfering RNA (siRNA) and short hairpin RNA (shRNA). For siRNA, various concentrations were used in combination with the siQuest reagent (20 μ l). The siRNA was used at the following final concentrations: 0, 50, 100, 200, or 300 nM in the low bicarbonate DMEM and 10% FCS and applied to the cells. Double-stranded RNA (dsRNA) was from Applied Biosystems (Foster City, CA) as "select validated." For Grb2 silencing, we used a dsRNA that targeted exons 3 and 6, sense sequence 5'-GGCAGAACUCAUUGGGAAAtt-3' (H, thymine-thymine overhangs introduced by the manufacturer to increase the efficiency of the small interfering RNAs [siRNAs]). The cells were allowed to incubate with the siRNA in complete medium (minus antibiotics) for 3 days before being harvested. The method of silencing using shRNA specific for Grb2 was performed as described in reference 6.

PI5K was silenced using siRNA similar to Grb2 siRNA, as detailed above. The dsRNA was obtained from Applied Biosystems (Foster City, CA) as select validated. For PI5K silencing, we used a dsRNA that targeted exon 7, sense sequence 5'-CAAGAUCGGUAAAAAUGCAAtt-3'.

Phagocytosis assays. Phagocytosis was measured in the LR5/RAW lines by using fluorescent-labeled green fluorescent protein (GFP) zymosan A (*Saccharomyces cerevisiae*) (Invitrogen, Carlsbad, CA). The particles were opsonized at 37°C for 1 h using the zymosan A BioParticles opsonizing reagent (derived from highly purified rabbit polyclonal IgG antibodies) (Invitrogen, Carlsbad, CA) and were applied to approximately 1×10^7 cells such that there were 20 zymosan particles per each cell. After application of the Zymosan, the 6-well plates containing the cells were sedimented at 800 \times g for 5 min and then were incubated at 37°C for 15 min. Fluorescent-labeled zymosan particles ingested by the cells were counted manually in three different fields.

For phagocytosis assays intended for fluorescence microscopy, sheep red blood cells (RBCs) (Colorado Serum, Denver, CO) were opsonized with rabbit anti-sheep red blood cell IgG from Diamedix (Miami, FL). To synchronize phagocytosis, the opsonized RBCs were added to cells at 4°C in BWD buffer (20 mM HEPES, pH 7.5, 125 mM NaCl, 5 mM KCl, 5 mM dextrose, 10 mM NaHCO₃, 1 mM KH₂PO₄, 1 mM CaCl₂, 1 mM MgCl₂) for least 15 min and then elevated to 37°C for 5 min as described in reference 25.

PIP₂ and PA liposome preparation. PA was prepared as DOPA (1,2-dioleoyl-sn-glycero-3-phosphate; Avanti Polar Lipids, Alabaster, AL) and was prepared by resuspending 1 mg DOPA in 1.4 ml liposome buffer (1 \times PBS plus 0.5% bovine serum albumin [BSA], pH 7.2). The solution was diluted in low bicarbonate DMEM plus 10% FCS to achieve an intermediate stock of 1 mM and then sonicated at medium strength for 20 bursts of 5 s each while on ice. Intermediate dilutions were made in Hanks' balanced buffer plus 0.5% BSA, pH 7.35, and

applied to the cells. PIP₂ was prepared by drying under a N₂ stream to evaporate the Cl₃CH and resuspending in liposome buffer, following the protocol as indicated above for PA.

Immunofluorescence microscopy. Approximately 1×10^5 RAW/LR5 cells were transfected with fluorescence chimeras Cerulean-C1-Grb2-WT, Citrine-C1-PLD2-WT or both. After 48 h, cells were plated onto round glass coverslips in a 24-well plate and were cultured overnight at 37°C with 5% CO₂ in RPMI medium with 10% fetal bovine serum. Phagocytosis was conducted as indicated in reference 25. The cells were fixed with 3.7% formaldehyde, permeabilized (0.2% Triton X-100), and were then stained to determine F-actin using phalloidin conjugated with Alexa Fluor 568. The fluorescent signals from yellow fluorescent protein (YFP)-PLD2 and from cyan fluorescent protein (CFP)-Grb2 were detected with YFP and CFP filters, respectively. All images were taken using the 60 \times magnification with the OIL/1.40 phase 3 objective of an Olympus IX71 microscope coupled to a SensiCam cooled charge-coupled device camera. Quantitation of phagocytic cups was based on the presence of actin-rich cup formation in the far-red channel (568 nm) for actin as described in reference 25.

Statistical analyses. Data are presented as the means \pm the standard errors of the means (SEMs). The difference between means was assessed by the single-factor analysis of variance (ANOVA) test or by the Student *t* test, as indicated in the legends of the figures. In either case, a probability of *P* < 0.05 was considered to indicate a significant difference.

RESULTS

WASp, PLD2, and Grb2 are colocalized to the early phagocytic cup. It is known that PLD2 plays an important role during phagocytosis, yet the mechanism for how this is accomplished is far from being understood (13). Our laboratory has shown previously that PLD2 is a key protein during chemotaxis mediated by ancillary proteins such as Grb2 (15, 16). We began this study by hypothesizing that Grb2 could also mediate the effect of PLD2 on phagocytosis. RAW/LR5 cells, previously transfected with GFP-Grb2 and myc-PLD2, were exposed to RBCs opsonized with IgG antibodies, and Fig. 1A shows a macrophage engulfing a single RBC (arrowhead) with clear colocalization of PLD2, Grb2, and actin at the point of contact. The results in Fig. 1B indicate that the WASp and PLD2 proteins are both present in the early phagocytic cups along with F-actin. The arrowheads in Fig. 1B point toward nascent phagocytic cups, where actin, WASp, and PLD2 are all colocalized. Figure 1B highlights the migration of WASp to the phagocytic cup, which is normally a cytosolic protein but during periods of early phagocytosis is localized alongside PLD2 to the site of contact with the RBC being engulfed. Figure 1C demonstrates colocalization of Grb2 and WASp to the membrane. Once again, this figure demonstrates the normally cytosolic WASp being localized to the point of contact with the target (RBC) and demonstrates that both WASp and Grb2 are colocalized around the RBC (arrowhead) as it becomes engulfed by the macrophage. As Fig. 1A (PLD2 and Grb2), Fig. 1B (PLD2 and WASp), and Fig. 1C (Grb2 and WASp) represent pairings of two proteins, we next investigated the presence of all three proteins (PLD2, Grb2, and WASp) simultaneously localized at the phagocytic cup. Figure 1D demonstrates the presence of all three component proteins (PLD2, Grb2, and WASp), which are all localized to the nascent phagocytic cup and are seen forming a ring around the RBC (arrowhead) as it becomes engulfed by the macrophage. In summary, these immunofluorescent images demonstrate the strong presence of PLD2, WASp, and Grb2 in nascent phagocytic cups during early phagocytosis.

Grb2 and PLD2 bind together in living cells. To better understand how PLD2, Grb2, and WASp interact, coimmuno-

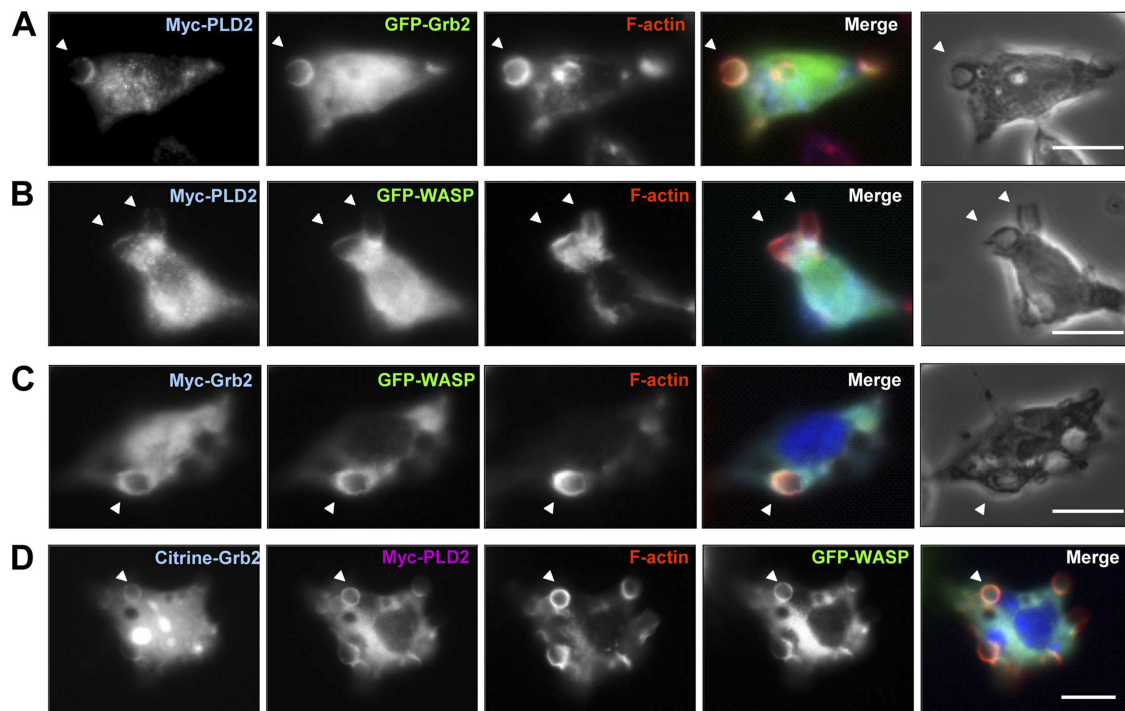


FIG. 1. Colocalization of WASp, Grb2, and PLD2 in the phagocytic cup. LR5 cells were cotransfected using combinations of myc-PLD2 and GFP-Grb2 (A), myc-PLD2 and GFP-WASp (B), or myc-Grb2 and GFP-WASp (C) or were triply transfected with citrine-Grb2, myc-PLD2, and GFP-WASp. All cells were stained with F-actin using Alexa 647-phalloidin and the presence of myc using mouse anti-myc, followed by Alexa 568-anti-mouse antibody. (A) Myc-PLD2 (cyan), GFP-Grb2 (green), and F-actin (red) were seen in the phagocytic cup surrounding the RBC (merge panel, indicated by an arrowhead). (B) Myc-PLD2 (cyan), GFP-WASp (green), and F-actin (red) were visualized at the phagocytic cup during engulfment of RBCs (merge panel, indicated by arrowheads). (C) Myc-Grb2 (cyan), GFP-WASp (green), and F-actin (red) were visualized at the phagocytic cup (indicated by an arrowhead). (D) Triply transfected LR5 cells were probed for Citrine-Grb2, myc-PLD2 (magenta), GFP-WASp (green), and F-actin (red). WASp, PLD2, and Grb2 were seen in the phagocytic cup during initial engulfment (indicated by an arrowhead). The rightmost panels of panels A, B, and C show the phase-contrast images for the corresponding fields. Bar, 10 μ m.

precipitations were performed using groups of cells cotransfected with two plasmids, one encoding PLD2 (see protein architecture in Fig. 2A) and one encoding Grb2 (see protein architecture in Fig. 2C). In Fig. 2B, the top two panels represent positive controls showing appropriate expression of transfected myc-tagged PLD2 and YFP-tagged Grb2 proteins. The third and fourth panels from the top in Fig. 2B demonstrate that PLD2 and Grb2 are associated in the cell as each protein can both be immunoprecipitated (IP) with antibodies specific for the other protein (IP for Grb2 and WB for myc-PLD2 or IP for myc-PLD2 and WB for YFP-Grb2). The bottom panel represents a control to show equal loading in all lanes by using an antibody for β -actin. These data demonstrate an association between PLD2 and Grb2 within the cell.

Disruption of the PLD2-Grb2-WASp association with PLD2 mutant proteins. The experiments described above demonstrate an association between the PLD2 and Grb2. Our working hypothesis for the next set of experiments was that we could disrupt PLD2 binding to Grb2 and also disrupt Grb2 binding to PLD2 by using various mutant isoforms of these two proteins in place of the wild-type proteins used in the previous experiment. A PLD2-Grb2 interaction would involve the single SH2 motif on Grb2 and the two SH2-targeted tyrosine residues on PLD2.

For the first binding scenario between PLD2 and Grb2 (the SH2 domain on Grb2), we utilized the Grb2-R86K mutant that

hinders and disables binding of the Grb2 SH2 domain to its targets (PLD2). The Grb2-R86K mutant demonstrated no binding with PLD2 during a pull-down for PLD2 (Fig. 2D), as IP with anti-Xpress antibody and subsequent WB analysis with anti-myc antibody did not pull-down the myc-tagged PLD2 protein and resulted in no binding between PLD2 and the Grb2-R86K mutant (Fig. 2D, third panel from the top). Additionally, the inverse binding interaction that utilized IP with an anti-myc antibody and subsequent WB analysis with anti-Xpress antibody did not pull down the Xpress-tagged Grb2 protein (Fig. 2D, fourth panel from the top) and also alternatively resulted in no binding between Grb2-R86K and PLD2.

For the second binding scenario between PLD2 and Grb2, two different tyrosine residues on PLD2 can be bound by the SH2 domains of Grb2. These are the phosphorylated Y-169 and Y-179 (see schemes depicted in Fig. 2E and Fig. 2G, respectively) (7). As seen in Fig. 2F, the mutant PLD2-Y169F protein is only marginally capable of binding to Grb2, as IP with anti-Xpress antibody and subsequent WB with α -myc antibody only marginally pulled down the myc-tagged PLD2 protein associated with the Xpress-tagged Grb2 (Fig. 2F, third panel from the top). We document that binding of Y169F to Grb2 is decreased by \sim 70%, which is in accordance with the cell biology data presented later in this paper. In Fig. 2H, the mutant PLD2-Y179F protein showed a complete loss of binding between Grb2, as IP with anti-Xpress antibody and subse-

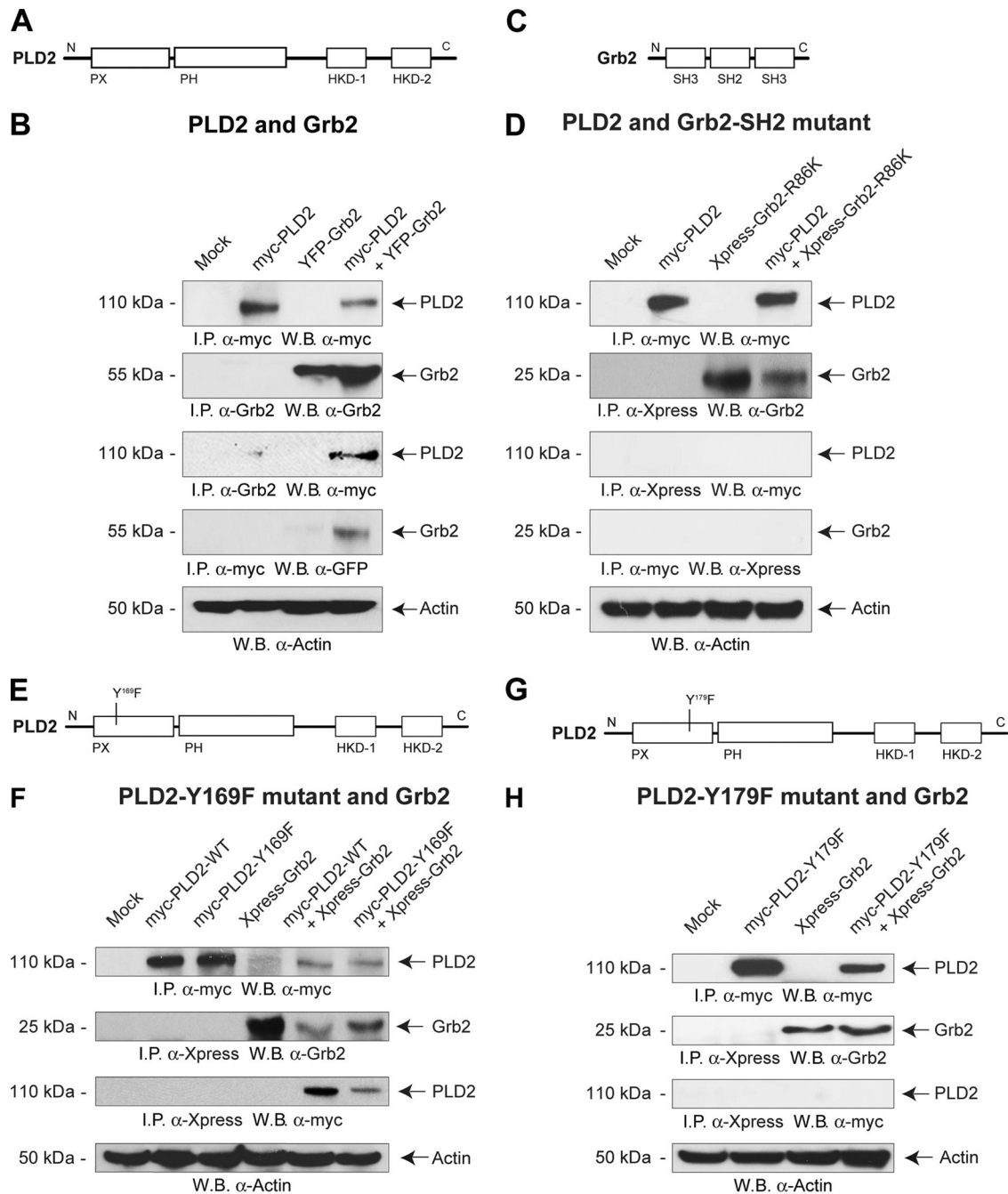


FIG. 2. Disruption of binding between PLD2 and Grb2 using PLD2 mutants (PLD2-Y169F and PLD2-Y179F) or the Grb2-SH2 mutant. Schematic diagrams with domain composition of PLD2-WT, PLD2-Y169F, PLD2-Y179F, and Grb2-WT are shown in panels A, E, G, and C, respectively. (B) Cells were transfected with either myc-PLD2 or YFP-Grb2, alone or in combination. (D) Cells were transfected with either myc-PLD2 or Xpress-Grb2-R86K, alone or in combination. (E) Cells were transfected with myc-PLD2-WT, PLD2-Y169F, or Xpress-Grb2, alone or in combinations. (H) Cells were transfected with myc-PLD2-Y179F or Xpress-Grb2, alone or in combination. Cells were harvested 48 h posttransfection, and lysates were immunoprecipitated (IP) and subjected to Western blot (WB) analysis with the indicated antibodies. (B, D, F, and H) The top two panels represent positive controls (immunoprecipitation and immunoblotting with the same antibody), and the bottom panel is the control that shows an approximately equal amount of protein in the lysates used for the immunoprecipitation, as ascertained with antiactin antibodies.

quent WB with anti-myc antibody did not pull down the myc-tagged PLD2 protein and resulted in no binding between Grb2 and the Y179F mutant (Fig. 2F, third panel from the top).

A Grb2-WASp interaction would involve the SH3 domains in Grb2 (Fig. 3C) and would bind to the poly-proline target in

WASp (Fig. 3A). Figure 3B shows the association between WASp and Grb2. The top two panels in Fig. 3B are positive controls showing appropriate expression of transfected YFP-tagged Grb2 and untagged WASp proteins. The third panel from the top in Fig. 3B demonstrates that Grb2 and WASp are

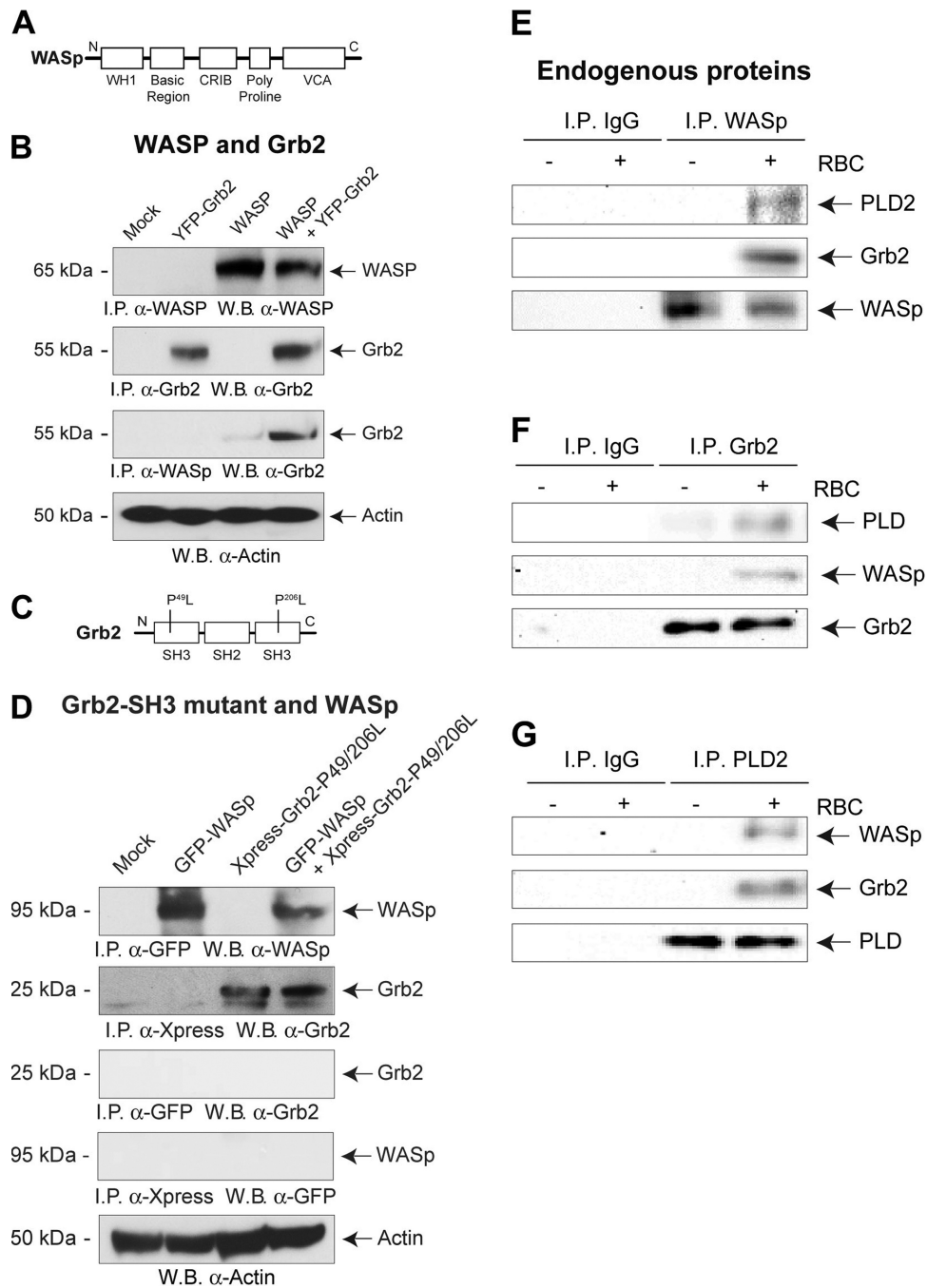


FIG. 3. Interaction between WASp and Grb2 is affected in the presence of the Grb2-SH3 mutant. (A and C) Schematic diagram showing domain composition of WASp (A) and Grb2-P49/206L (C). (B) Cells were transfected with either YFP-Grb2 or WASp, alone or in combination. (D) Cells were transfected with either GFP-WASp or Xpress-Grb2P49/206L, alone or in combination. Cells were harvested 48 h posttransfection, and lysates were immunoprecipitated and subjected to WB analysis with the indicated antibodies. (B and D) The top two panels are positive controls (IP and WB analysis with same antibody), and the bottom panel is the control that shows an approximately equal amount of protein in the lysates used for the immunoprecipitation, as ascertained with antiactin antibodies. (E to G) PLD2, Grb2, and WASp interact at endogenous levels. RAW 264.7 cell lysates were immunoprecipitated in the presence and absence of RBCs with anti-WASp (E), anti-Grb2 (F), or PLD2 (G) antibodies, respectively, and probed for PLD2, Grb2, and WASp in each case. The two left lanes of each panel represent immunoprecipitation with IgG antibody in the presence and absence of RBCs, and thus serve as negative controls.

associated in the cell as immunoprecipitation with an α -WASp antibody and WB analysis using an anti-Grb2 antibody pulled down the associated Grb2 protein. This protein-protein interaction between WASp and Grb2 can be disrupted when the

two SH3 domains on Grb2 are simultaneously hindered through the use of the Grb2-P49/206L double mutant, which disables binding to its polyproline targets (Fig. 3C). As shown in Fig. 3D, the Grb2-P49/206L double mutant demonstrated

no binding with WASp during a pull-down for Grb2 (Fig. 3D), as IP with anti-GFP antibody and subsequent WB analysis with anti-Grb2 antibody did not pull-down the Xpress-tagged Grb2 protein and resulted in no binding between WASp and the Grb2-P49/206L mutant (third panel from the top). Additionally, the inverse binding interaction that utilized IP with an anti-Xpress antibody and subsequent WB with anti-GFP antibody did not pull-down the GFP-tagged WASp protein (Fig. 3D, fourth panel from the top) and also alternatively resulted in no binding between Grb2-P49/206L and WASp.

Data shown in Fig. 2A to H and in Fig. 3A to D, respectively, indicate that Grb2 utilizes its SH2 to bind to PLD2 and its two SH3 domains to bind to WASp. The results of the immunoprecipitations and Western blots using two-by-two pairs of proteins depicted in Fig. 2 and 3 allowed us to hypothesize the occurrence of the trimeric complex PLD2-Grb2-WASp *in vitro*. The previous experiments were repeated with endogenous proteins from macrophages to rule out any artifact that might have caused nonspecific associations in overexpressed cells. Murine macrophages were stimulated with IgG-opsonized RBCs, and data presented in Fig. 3E to G show the formation of the PLD2-Grb2-WASp trimeric complex (right lanes), which increased following stimulation regardless of the antibody that was used for immunoprecipitation (Fig. 3E, WASp IP; Fig. 3F, Grb2 IP; or Fig. 3G, PLD2 IP). Using immunofluorescence microscopy and immunoprecipitations, we document the formation of the PLD2-Grb2-WASp heterotrimeric protein complex in both endogenous and transfected cells.

PLD2 and WASp bind together via a Grb2-mediated interaction, and silencing Grb2 prevents the PLD2-WASp association. We were able to detect a PLD2-WASp protein-protein interaction using GFP-tagged WASp and myc-tagged PLD2. As shown in Fig. 4A, the top two panels are positive controls showing appropriate expression of transfected myc-tagged PLD2 and GFP-tagged WASp proteins. The third and fourth panels from the top in Fig. 4A demonstrate that PLD2 and WASp are associated in the cell, as each protein can be immunoprecipitated with antibodies specific for the other protein (IP for myc-PLD2 and WB for WASp or IP for WASp and WB for myc-PLD2). The bottom panel is a control to show equal loading in all lanes using an antibody for β -actin. These data demonstrate an association between WASp and PLD2 within the cell, which is mediated by the third protein partner, Grb2. As presented in Fig. 4B, both PLD2 and WASp do indeed interact in the presence of endogenous Grb2 (left lanes of the second and third panels from the top), as shown when either PLD2 or WASp was immunoprecipitated and then probed in the subsequent Western blot analysis using an antibody specific for the other protein (WASp or PLD2). However, we hypothesized that this PLD2-WASp interaction is mediated by Grb2 acting as a “docking” protein. To investigate this, we silenced Grb2 with small interfering RNA (siRNA) specific for Grb2 (siGrb2). Endogenous PLD2 and WASp were then coimmunoprecipitated to determine whether they still interacted in the absence of Grb2. As shown in Fig. 4B, the decrease in the interaction between PLD2 and WASp (second panel from the top) is decreased by >30% at the highest concentration of siGrb2 used (right lanes), while the inverse interaction (second panel from the bottom) is decreased ~70% at the highest concentration of siGrb2 used (also right lanes). The results

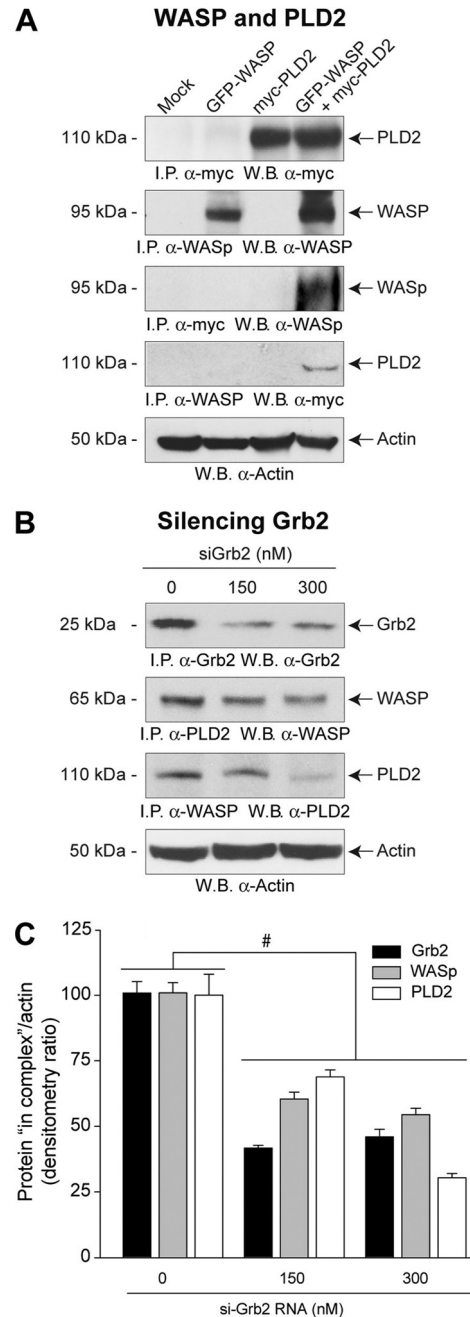


FIG. 4. Interaction between WASp and PLD2 is affected when endogenous Grb2 is silenced. (A) Cells were transfected with GFP-WASp or myc-PLD2WT, alone or in combinations. Cells were harvested 48 h posttransfection, and lysates were immunoprecipitated and subjected to WB analysis with the indicated antibodies. The top two panels are positive controls (IP and WB analysis with same antibody), and the bottom panel is a control that shows equal loading in all lanes as ascertained with antiactin antibodies. (B) Endogenous Grb2 was silenced with the indicated amount of siGrb2 RNA. Three days post-silencing, the cells were harvested and the lysates were immunoprecipitated and subjected to WB analysis with the antibodies indicated. The bottom panel is the actin control showing equal loading. (C) Quantification of protein expression in the PLD2-Grb2-WASp complex in relation to actin. Data represent means \pm SEMs of three independent experiments. The difference between means was assessed by the single-factor analysis of variance (ANOVA) test, and # denotes a significant decrease ($P < 0.05$) in intensity compared to that of the control.

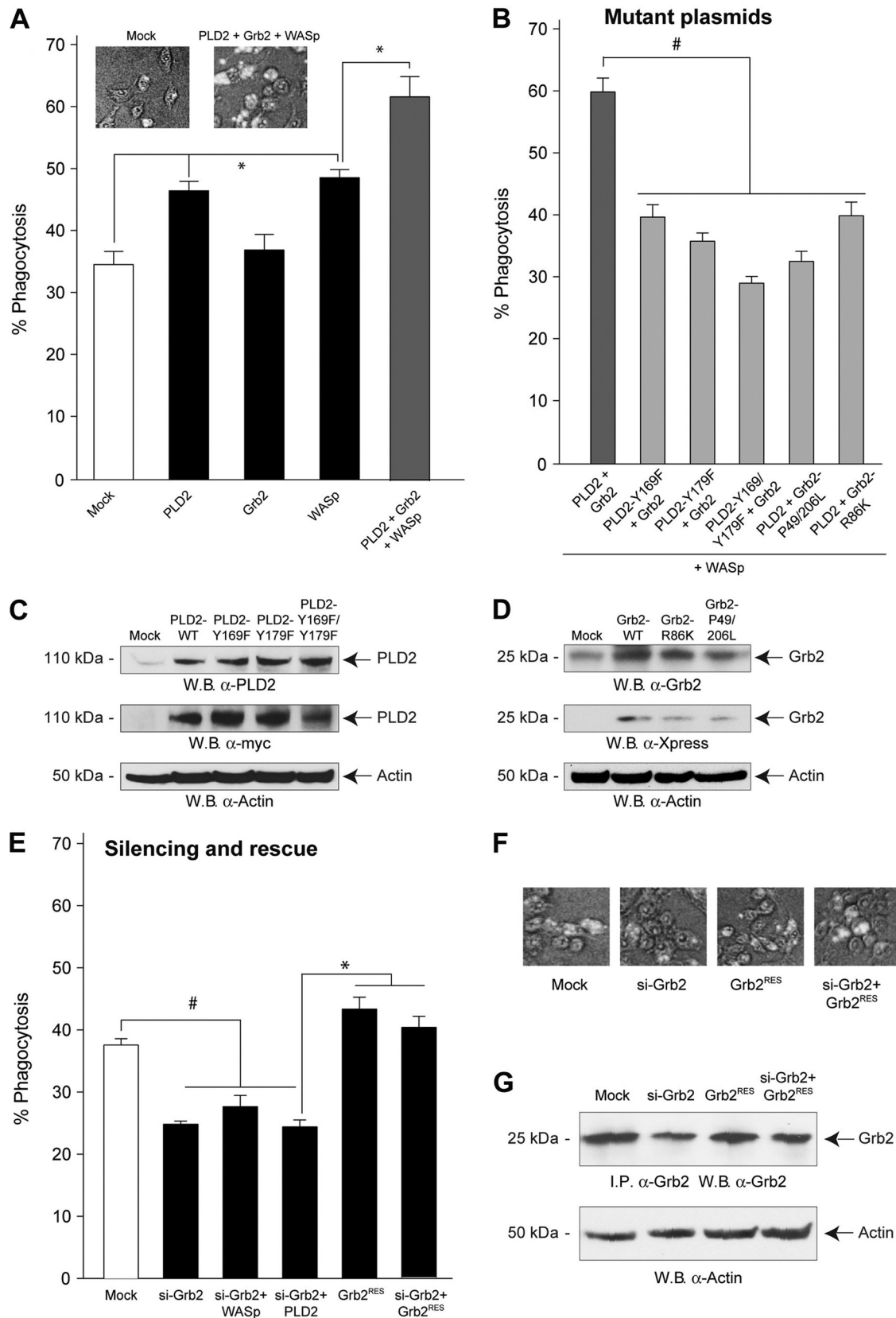


FIG. 5. PLD2-Grb2-WASp heterotrimer enhances phagocytosis. RAW264.7 macrophages were transfected with combinations of PLD2, WASp, Grb2, and various mutant plasmids to study the effect on phagocytosis. (A) Cells were either singly or triply transfected with combinations of PLD2-WT, Grb2-WT, and WASp-WT. The inset shows micrographs of typical fields with fluorescent beads phagocytosed by macrophages.

presented in Fig. 4B and its quantification shown in Fig. 4C indicate that binding was significantly diminished under conditions in which Grb2 was increasingly silenced, thus confirming the role of Grb2 as the “glue” between PLD2 and WASp.

Grb2 and PLD2 are upstream effectors of WASp activation and subsequent WASp-mediated phagocytosis. To ascertain the physiological effects the heterotrimer has on macrophages, phagocytosis assays were performed using mouse RAW264.7 macrophages overexpressing the three proteins of interest. Mock transfection demonstrated a basal level of phagocytosis at 35 to 40% (Fig. 5A), which was modestly increased (~50% above basal level) in the presence of either PLD2 or WASp but not with Grb2. The triple-transfected condition (PLD2 plus Grb2 plus WASp) showed an almost 2-fold increase in phagocytosis.

To determine whether or not the binding of PLD2 or Grb2 had an effect on phagocytic activity, mutant isoforms of PLD2 and Grb2 were cotransfected into the triple transfections, replacing their respective wild-type isoform (Fig. 5B). The results indicate that expression of the Grb2-R86K mutant, and even more so the Grb2-P49/206L mutant, failed to provide the robust increase in phagocytosis observed in Fig. 5A. Likewise, a lack of enhanced phagocytosis was observed with the PLD2-Y169F or PLD2-Y179F mutant, and the double mutant PLD2-Y169/179F led to a profound decrease in phagocytosis. Diminished phagocytosis, seen in Fig. 5B, is a result of the intrinsic dominant negative nature of the PLD2 and Grb2 mutants, which is not due to a lowered level of PLD2 or Grb2 protein expression, since all recombinant PLD2 and Grb2 proteins are similarly expressed, as shown in Fig. 5C (PLD2) and Fig. 5D (Grb2), respectively. The mutants are indeed dominant negative, as experiments using 1.5 μ g DNA show, and the level of phagocytosis is below that of controls, particularly for certain mutants. We do not believe that endogenous proteins compete for the effect of the mutants, and given the high levels of overexpression, endogenous proteins should not be able to compensate. As for whether overexpression of individual mutants in the absence of WASp overexpression inhibits phagocytosis, we believe that they do.

As Grb2 silencing altered binding (Fig. 4B), we next wondered if silencing Grb2 could also alter phagocytosis. As shown in Fig. 5E, siGrb2 resulted in significant decreases in phagocytosis of macrophages alone or with subsequent overexpression of either WASp or PLD2. The results of this experiment implicate the importance of Grb2 in WASp-PLD2-mediated phagocytosis. To complement and validate the silencing experiments, we performed an experiment with a rescue plasmid

that was engineered to be resistant to silencing of Grb2 by siRNA via introduction of six silent mutations (Grb2^{RES}) (6). The results are presented in Fig. 5E (phagocytosis), Fig. 5F (representative micrographs of engulfed fluorescent beads), and Fig. 5G (Western blots showing protein expression levels) and indicate that in the experimental conditions used for silencing Grb2, phagocytosis could be rescued and full restorations of physiological effects could be demonstrated.

Disruption of interaction with PLD2 and Grb2 cripples phagocytic cups. Results from experiments shown in Fig. 1 demonstrate that PLD2, WASp, and Grb2 colocalized to the phagocytic cup during engulfment of a particle. Experiments shown in Fig. 2 and Fig. 3A to D, respectively, indicate that the PLD2 and Grb2 mutants alter binding to their respective targets. Therefore, we next investigated if these same mutated proteins could also alter the formation of the phagocytic cup, specifically in the early phagocytic cup (surrounding the engulfed RBC). To determine whether this hypothesis was correct, mutant isoforms of PLD2 were transfected into macrophages and immunofluorescence images were generated in Fig. 6A. The top row of images (PLD2-WT) shows a robust formation of cups, as evidenced by the total engulfment of the RBC by the macrophage. The second and third rows from the top (PLD2-Y169F and PLD2-Y179F, respectively) show a somewhat deficient formation of cups, as the RBCs are not completely engulfed, and the bottom row (PLD2-Y169F/Y179F) shows a reduced and minimal cup formation and no engulfment of the RBCs. The immunofluorescent images were also quantified by counting the number of cups per cell, which is presented in Fig. 6B and demonstrates the negative effect of the PLD2 double mutant (PLD2-Y169F/Y179F) on cup formation whether in the presence of overexpressed Grb2 or WASp. Single mutations in PLD2 (Y169F or Y179F) demonstrate a small but significant reduction in the number of cups, but the double mutant causes the greatest decrease in the number of cups. This is in accordance with the immunofluorescent images shown in Fig. 6A. Figure 6C shows that when WASp was overexpressed in the presence of PLD2-Y169F/Y179F, there is minimal formation of cups (only one cup in the panel) with some recruitment of PLD2 and also WASp. These data indicate that phagocytosis or cup formation is inhibited approximately 50% with PLD2 mutants that impair the ability of the phospholipase to bind to Grb2 and, therefore, subsequently recruit WASp to the heterotrimer. Even though there is some localization, the PLD2-Y169F/Y179F double mutant shows a less-efficient effect than PLD2-WT. We believe this effect is more quantitative than qualitative.

(B) Cells were triply transfected with combinations of PLD2-WT or mutant PLD2 (PLD2-Y169F or PLD2-Y179F or PLD2-Y169/179F), Grb2-WT, or mutant Grb2 (Grb2-R86K or Grb2P49/206L) and WASp-WT, and the effect on phagocytosis was examined. Percent phagocytosis is indicated. (C and D) Western blot analyses with indicated antibodies showing the expression of PLD2-WT, PLD2Y169F, PLD2Y179F, or PLD2-Y169/179F (C) and Grb2-WT, Grb2-R86k, or Grb2-P49/206L (D). Bottom panels are actin controls that show equal loading in all lanes. (E to G) Cells were transfected with siRNA specific for silencing Grb2 protein expression. Cells silenced for Grb2 were transfected with either PLD2 or WASp, or they were first silenced and then transfected with a rescue plasmid for Grb2 (pcDNA-XGrb2^{RES}-WT). (E) Cells were examined for phagocytosis after 3 days of transfection. Percent phagocytosis is indicated. (F) Micrographs of corresponding fields indicated with fluorescent beads phagocytosed by macrophages. (G) Western blot showing Grb2 protein levels after silencing and rescuing treatments (the actin panel shows equal gel loading). Percent phagocytosis is measured as the number of cells that had engulfed particles out of the total number of cells in the examined field \pm SEMs for four different fields, and the difference between means was assessed by ANOVA. * denotes a significant increase ($P < 0.05$) in intensity compared to the control, and # denotes a significant decrease ($P < 0.05$) in percent phagocytosis compared to that of the control.

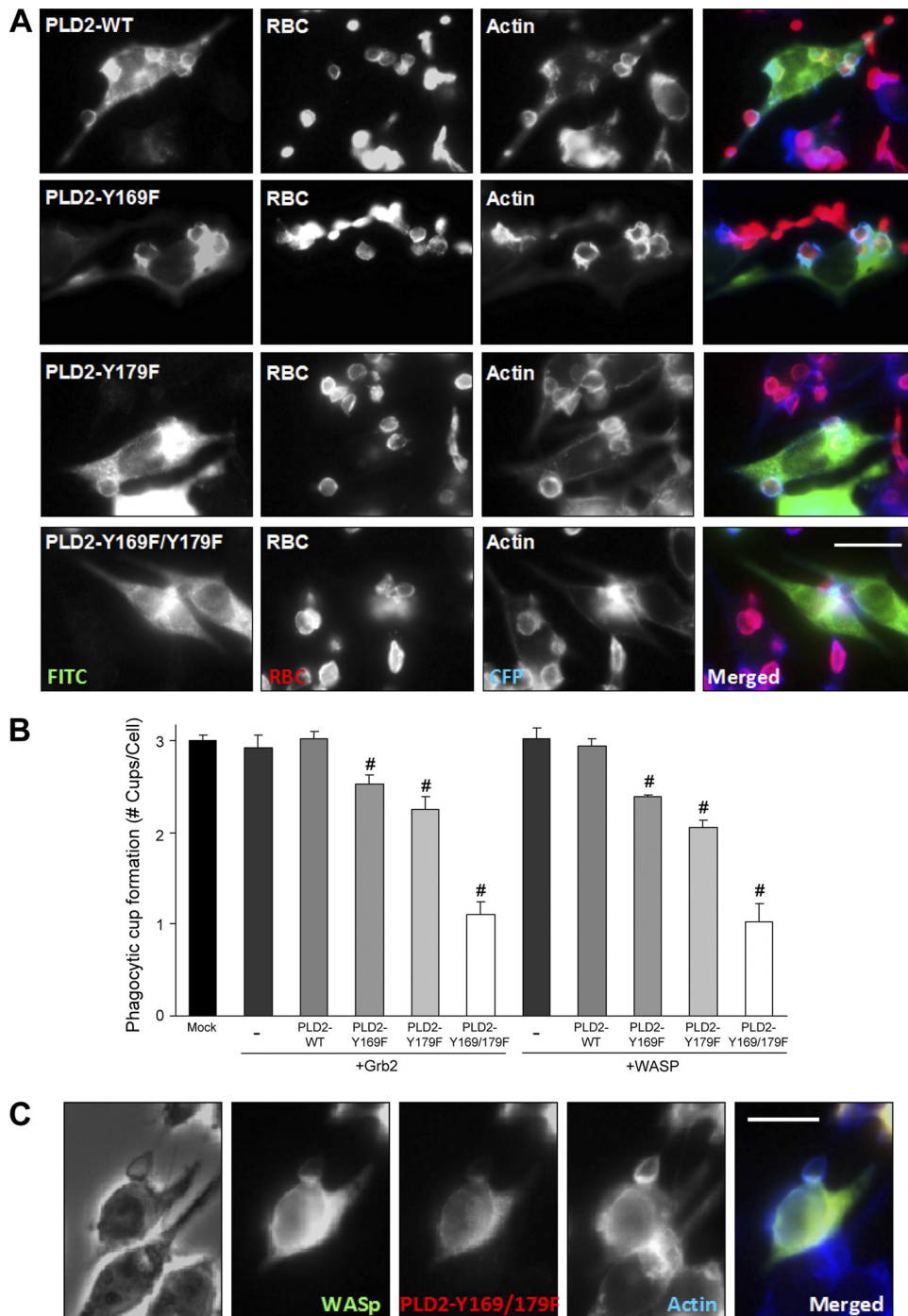


FIG. 6. Disruption of binding results in crippled phagocytic cup formation with PLD2 mutant plasmids. RAW/LR5 cells were transfected with the myc-PLD2-WT, Y169F, Y179F, or Y169F/Y179F mutant. (A) Transfected cells were exposed to opsonized RBCs (red) after 2 days, and the cells were stained with anti-myc followed by Alexa 488–anti-mouse (green), Alexa 568–anti-rabbit (RBCs) (red), and Alexa 647-phalloidin (cyan) antibodies. (B) Quantitation of immunofluorescence images (from panel A) showing the average number of cups per cell. Over 30 cells were examined per experiment, and three independent experiments were analyzed. Data represent the means \pm the SEMs of three independent fields; # denotes a significant decrease ($P < 0.05$) in phagocytic cup formation compared to that of the control. The difference between means was assessed by ANOVA. (C) Overexpression of myc-PLD2-Y169F/Y179F and GFP-WASp and derived immunofluorescence images.

PLD2 has a double role in the PLD2-Grb2-WASp complex. We next investigated if PLD2 enzymatic activity (production of PA) was responsible for the observed effect in phagocytosis. We first analyzed inhibition of endogenous PLD (Fig. 7A,

black bars) in macrophages using two different PLD inhibitors (FIPI and CAY10594) (28, 29) and found that phagocytosis was inhibited by both small molecules. Second, we overexpressed PLD2 (Fig. 7A, gray bars) and found that the phago-

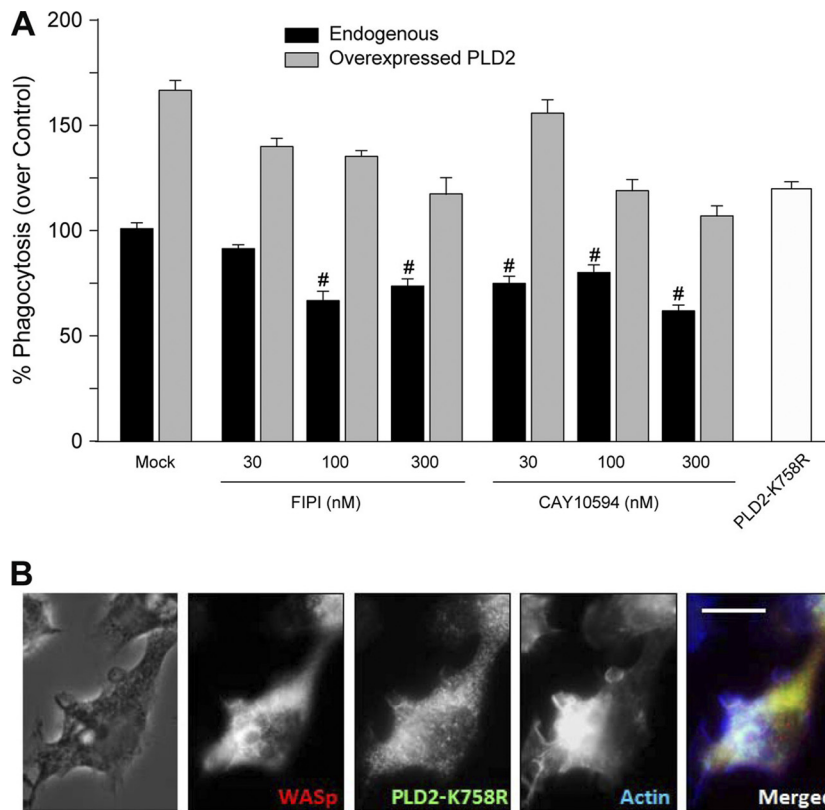


FIG. 7. Role of PLD2 catalytic activity in phagocytosis. (A) Cells were incubated with increasing concentrations of PLD2 inhibitors (FIPI and CAY10594) to inhibit levels of endogenous PLD2 (black bars) or cells overexpressing PLD2 for 2 days (gray bars) prior to incubation with inhibitors. In either case, cells incubated with inhibitors were assayed for phagocytic activity. Cells transfected with a catalytically inactive mutant, PLD2-K758R (white bar), served as the control for this experiment. Data represent means \pm SEMs of three independent fields; # denotes a significant decrease ($P < 0.05$) in percent phagocytosis compared to that of the control. The difference between means was assessed by ANOVA. (B) Immunofluorescence images of the YFP-PLD2-K758R mutant transfected with myc-WASp.

cytosis component due to recombinant PLD2 is also inhibited by FIPI and CAY10594. In both cases, phagocytosis is never completely inhibited (only 40 to 60%). Furthermore, the lipase-inactive mutant PLD2-K758R also enhanced phagocytosis by 50%, as shown in the last column of Fig. 7A (but still the level of phagocytosis is not as high as it is with the wild type). Figure 7B indicates that the formation of cups is still possible in cells transfected with PLD2-K758R and WASp, although the number is reduced compared to that for PLD2-WT (Fig. 6A and B). These results indicate that phagocytosis or cup formation is reduced approximately 50% when PLD2 is reduced (either through the use of small molecule PLD2 inhibitors or through the use of the catalytically inactive PLD2-K758R mutant).

Role of phospholipids in PLD2-Grb2-WASp phagocytosis.

Previous studies have shown activation of WASp to be reliant upon PIP₂, although those experiments were performed with purified proteins (27). To better understand the specific role that PLD2 has in the activation of WASp-mediated phagocytosis, we examined the effect of two of the downstream products of PLD2 activity, PA directly and PIP₂ indirectly through PA-mediated activation of PI5K (3) on phagocytosis of RAW264.7 macrophages *in vivo*. As shown in Fig. 8A, both PA and PIP₂ (alone or in combination) were able to activate phagocytosis and implicate PA or PIP₂ as positive cofactors for

phagocytosis. We used a cell-membrane-soluble chemical form of PA (dioleoylphosphatidic acid [DOPA]) that readily enters the cells and achieves activation of cell signaling (8, 17). It has been shown that the loss of PIP₂ disrupts the ability of WASp to act upon Arp2/3 and subsequently cause loss of actin nucleation (9, 11, 14, 20). In previous studies, the isoform PI(4,5)P₂ has been a proven activator of WASp function, where it binds to WASp's basic region (32) and activates WASp through the relief of the intramolecular protein interactions of the WA and GBD domains. The WA domain is the region that encompasses the WH2 domains and the acidic domain. The acidic region can also be found in the VCA domain, which is where Arp2/3 binds to promote actin assembly. PIP₂ eliminates this autoinhibition by enabling WASp's WA domain to interact with the Arp2/3 complex and actin (9, 24, 26). Low levels of PIP₂ result in an inactive WASp and prevent the interaction with Arp2/3, resulting in small amounts of actin formation and decreased phagocytosis.

In Fig. 8A, murine macrophages transfected with WASp were treated with either PA or one of three isoforms of PIP₂: PI(3,4)P₂, PI(3,5)P₂, or PI(4,5)P₂. PA allowed for a boost in phagocytosis in these cells, and PI(3,5)P₂, PI(4,5)P₂, and PI(3,4)P₂ allowed for increased phagocytosis, as well [although PI(3,4)P₂ had the smallest effect of the three]. This figure demonstrates the integral role of these phospholipids in WASp-mediated phagocytosis.

As for the mechanism of WASp activation, we present data

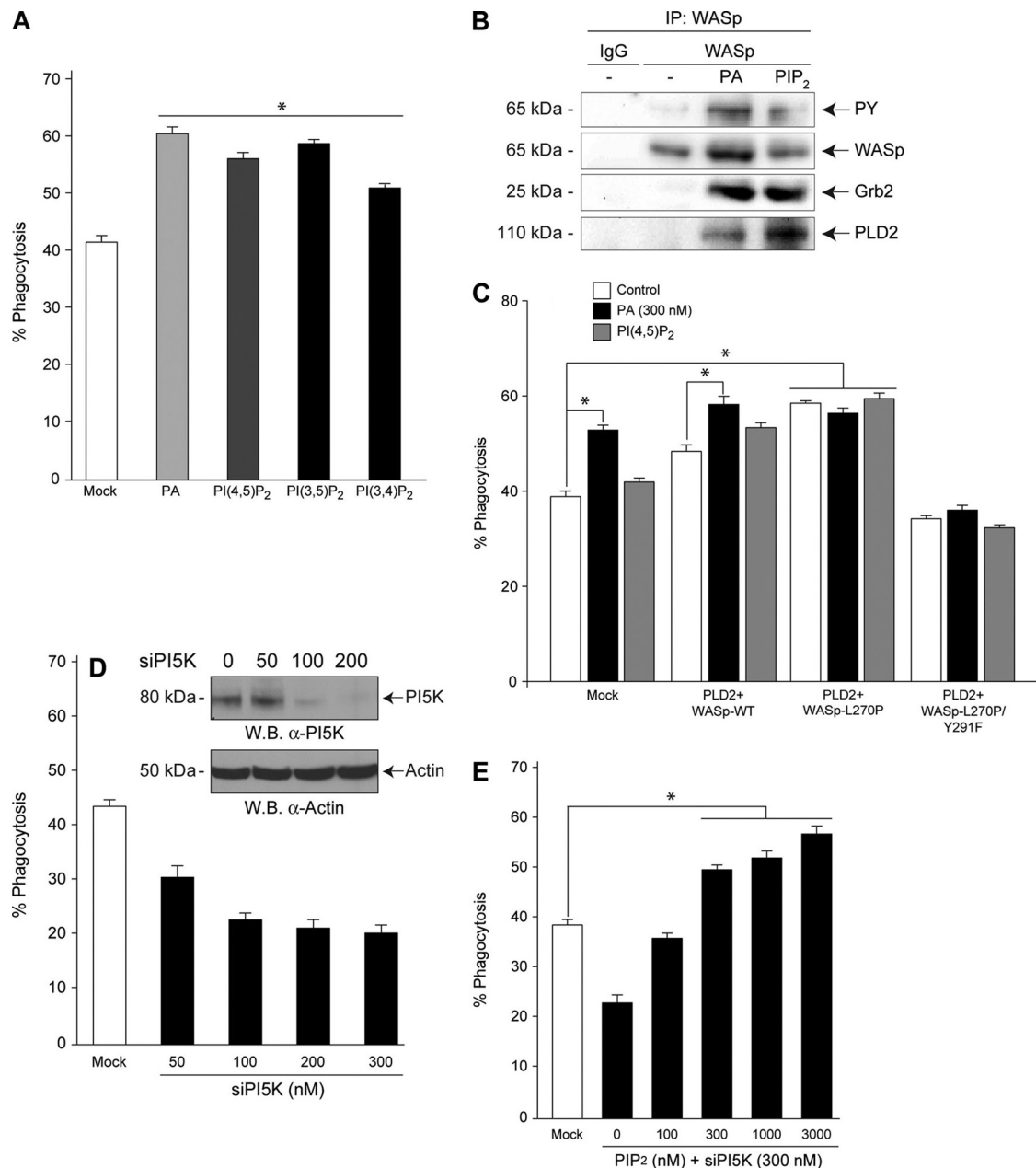


FIG. 8. Role of phospholipids in WASp-mediated phagocytosis. (A) RAW264.7 macrophages were transfected with WASp plasmid and were supplemented with PA (as dioleoylphosphatidic acid [DOPA]), PI(4,5)P₂, PI(3,5)P₂, or PI(3,4)P₂ for 30 min prior to phagocytosis, and percent phagocytosis is indicated. (B) PA and PI(4,5)P₂ enhanced WASp phosphorylation. Cells were treated with PA and PI(4,5)P₂, and WASp was immunoprecipitated. IP WASp was subjected to WB analysis with indicated antibodies to determine levels of phosphorylated WASp, total WASp, Grb2, and PLD2. (C) Cells were cotransfected with PLD2-WT and WASp-WT, WASp-L270P (“open conformation”; constitutively active) or WASp-L270P/Y291F (unable to be activated). Two days after transfection, cells were treated with 300 nM PA (black bars) or PI(4,5)P₂ (gray bars); the white bars represent untreated cells. Percent phagocytosis was measured. (D) PI5K expression was silenced in RAW264.7 macrophages, which were used for phagocytosis 3 days posttransfection, and the percent phagocytosis was measured. (D) Inset shows PI5K silencing was also analyzed via Western blot analysis. (E) Increasing PI(4,5)P₂ concentrations rescue phagocytosis of PI5K-silenced RAW264.7 macrophages. (A and C to E) Data represent means \pm SEMs of three independent fields. * denotes a significant increase ($P < 0.05$) in percent phagocytosis; # denotes a significant decrease in percent phagocytosis compared to that of the control. The difference between means was assessed by ANOVA.

showing that PA causes tyrosine phosphorylation of WASp (Fig. 8B). Treatment of cells with exogenously added PA and PIP₂ induces a complex between PLD2, Grb2, and activated WASp, as indicated by the increased level of WASp phosphorylation, which leads to increased phagocytosis (25).

Moving next to investigate the mechanism of PA on WASp, we used two WASp mutants as described in reference 25: WASp-L270P, which is structurally in an “open conformation” and is constitutively active, and WASp-L270P/Y291F, which cannot be phosphorylated and is,

therefore, constitutively inactive. As shown in Fig. 8C, PLD2-WT enhanced coexpressed WASp-WT phagocytosis by ~10%. In contrast to this, WASp-L270P increased phagocytosis to its maximal levels (almost 25% over controls). This suggested that when WASp-WT was overexpressed it was not entirely activated within the transfected macrophages, as an “additional step” or “regulator” was missing. The levels reached by the WASp-L270P mutants were also reached if WASp-WT- and PLD2-transfected cells were supplemented with PA or PIP₂ liposomes (Fig. 8C), implicating once again the role of phospholipids as the additional step or regulation. Interestingly, PIP₂ had no effect on raising either the constitutively active or inactive isoforms of WASp. This result indicates that the exogenous PIP₂ is not acting on any other endogenous regulator of phagocytosis. Since the result of this is a robust augmentation of phagocytosis, Fig. 8C highlights the active role of PLD2 in this macrophage function and provides an explanation of the mechanism. The last set of bars on Fig. 8C show that the functionally inactive WASp mutant L270P/Y291F is unable to drive phagocytosis even in the presence of PLD2 or PA, suggesting that PLD2 requires WASp to elicit phagocytosis.

To clarify that PLD2 is not generating PA that is then converted to DAG, we have included in Fig. 8C data which show that PLD2 is transfected along with WASp-WT, WASp-L270P (constitutively active), or WASp-L270P/Y291F (constitutively inactive). If the DAGK pathway was being utilized as opposed to a WASp pathway, then the results from Fig. 8 would be seen as an increase in phagocytosis compared to their non-PA-treated conditions. WASp-WT-transfected conditions increase phagocytosis, and when supplemented with PA the increase is even more. However, conditions transfected with WASp-L270P/Y291F reduce phagocytosis down from that of WASp-WT levels. Even when PA is supplemented, no increase in phagocytosis is seen. Again, if the DAGK pathway was being utilized here, the WASp pathway would be circumvented and phagocytosis would return to higher levels, yet it does not, indicating that endogenous PLC is not sufficient to significantly affect phagocytosis, at least not in the utilized macrophage line (RAW/LR5).

PLD-synthesized PA upregulates PI5K, leading to the production of PIP₂ (10). To verify the implication of PI5K, we used siRNA specific for PI5K. As the level of PI5K silencing increased, the phagocytosis of macrophages decreased concomitantly by >70% (Fig. 8D). This negative effect on phagocytosis is also supported by Western blot data from similarly treated lysates (Fig. 8D, inset). Importantly, this inhibitory effect on phagocytosis by silencing PI5K was rescued by the presence of exogenous PIP₂ (Fig. 8E).

DISCUSSION

We report here for the first time that a heterotrimeric protein complex exists between PLD2, Grb2, and WASp *in vivo*, which is integral to phagocytosis. This is the first ever observation of an interaction involving WASp and PLD2 in a Grb2-dependent manner. Data in this study also unveil the mechanism by which PLD2 acts upon phagocytosis by affecting WASp on two points: by anchoring WASp to the cell membrane via Grb2 by protein-protein interactions and also by the PLD2 enzymatic product PA, leading to the synthesis of PIP₂ through PI5K. Overall, our studies indicate that in the cells

overexpressing all three of these proteins, phagocytosis is significantly enhanced. This signifies an integral role in which the heterotrimer is best able to function when all three of its components are present in the cell.

To date, there are no reports of PLD2 being involved in WASp activation. However, the present study emphasizes that the contribution of PLD2 is crucial to the whole process. As previously shown, PLD1 and PLD2 have an effect on phagocytosis, and PLD is activated upon activation of the Fcγ receptor by leukocytes (13). This demonstration validates the link between receptor activation and PLD, which is necessary to understand our results, as PLD2 needs to undergo this first step with the concomitant production of PA. Other studies have highlighted the importance of PLD2's role at the membrane during early phagocytosis (4), and images shown in Fig. 1 are in agreement with that study. In addition, our data for the first time show that WASp is involved in PLD2-mediated phagocytosis.

Another interesting aspect in this study is PLD2-generated PA, which regulates synthesis of PIP₂, an allosteric regulator of WASp (1, 22). In previous studies, the isoform PI(4,5)P₂ has been a proven activator of WASp function, where it binds to WASp's basic region (32). PIP₂ eliminates autoinhibition of WASp by enabling its WA domain to interact with the Arp2/3 complex and actin, which otherwise would interact with the GBD domain within WASp itself. Low levels of PIP₂, therefore, result in an inactive WASp and yield small amounts of actin formation and decreased phagocytosis, which can be overcome due to its association with PLD2 via Grb2. Thus, PIP₂ efficiently activates WASp following its binding to Grb2 and PLD2.

WASp activation is more complex than previously believed (5, 6, 26, 27, 32). In an inactivated state, WASp exists in a closed conformation with the GBD region binding the cofilin homology domain in the carboxy terminus (14). The closed conformation of WASp prevents it from binding any of the aforementioned proteins involved in actin filamentation. Despite the abilities of Cdc42 and PIP₂ to activate WASp, recent studies have demonstrated that WASp inhibition is still possible even in the presence of Cdc42 and PIP₂ (32). Proteins containing SH3 domains, such as Nck, have been implicated as necessary cofactors in the presence of Cdc42 and PIP₂. The possible explanation for activation of WASp due to formation of the heterotrimer (PLD2-Grb2-WASp) is via the SH3 domains of Grb2, which might stabilize the poly-proline region of WASp and prevent autoinhibition of the protein. Also, Grb2 has been shown to be an important regulator of PLD2 due to its ability to localize to the plasma membrane (5, 7). The localization of these proteins at the formation of the cups also suggests that WASp may be activated upon delivery to the membrane by Grb2. Once Grb2 has bound PLD2 with WASp, WASp can bind membranous PIP₂ and activate itself. It has been suggested in the past that PIP₂ activation may be difficult to occur due to its limited presence in the cell (as it is membrane bound) (12). This is in agreement with other studies that implicate SH3-containing proteins as necessary regulators of WASp.

Results from the experiments with the mutant isoforms of PLD2 and Grb2 also highlight the importance of the structure and functions of the proteins during phagocytosis. The Grb2

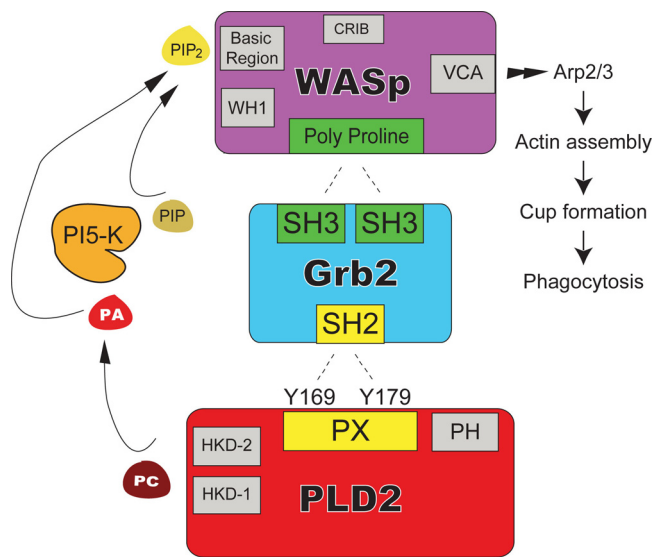


FIG. 9. Model of WASp activation. WASp is activated via two alternative pathways, a PLD2-mediated pathway and a Grb2-mediated pathway. First, PLD2 (bottom) catalysis of phosphatidylcholine (PC) via its two HKD lipase domains (bottom left) activates PI5K through PA, a product of PLD2. As a downstream product of PI5K, WASp (top) is activated by the subsequent PIP₂ produced by PI5K. Alternatively, Grb2 (middle) interacts with the polyproline region on WASp through its two SH3 domains, which then also results in WASp activation and leads to nucleation of actin filaments and to the formation of filopodia. Grb2 and PLD2 can physically interact with each other via two separate domains: the SH2 domain found on Grb2 binds to the PX domain on PLD2 (which contains the Y169 and Y179 motifs), which allows for Grb2 to function as the glue between WASp, membranous PLD2, and PIP₂. Furthermore, this method of WASp activation utilizes Grb2 as a stabilizer of the WASp polyproline motif, while PIP₂ stabilizes the WASp basic domain (top left), allowing the C-terminal WASp verprolin-cofilin-acidic (VCA) domain (top right) to act on the Arp2/3 complex and nucleate actin, which leads to enhanced phagocytosis.

domains required for binding (SH2 and SH3) must be present in order for the heterotrimer to form and function. All three protein components must be physically bound to one another in order for phagocytosis to occur, which is an effective way of regulating actin nucleation. Grb2 is able to bind and activate WASp, but only in the presence of a membranous cofactor, PIP₂. This represents a model wherein Grb2 acts as a “key” to activate WASp, and PIP₂ acts to turn the key to activate it and subsequently activate actin nucleation at the membrane. This method of WASp activation is a novel mechanism that is useful in preventing WASp from being activated arbitrarily in the cytosol.

The overall pathway is outlined in Fig. 9 and highlights the new discovery of the PLD2-Grb2-WASP trimer complex. This model also answers the mechanistic process: PLD2 would anchor the WASp-Grb2 dimer to the membrane and allow close proximity to regions where PIP₂ is abundant (as PLD-produced PA activates PIP5K that leads to its formation). This new model of WASp activation offers a method of actin nucleation dependent on PLD2, shedding new light on the dependency that cytoskeletal regulation has on this protein.

ACKNOWLEDGMENTS

Grants HL056653 (J.G.-C.) and GM071828 (D.C.) from the National Institutes of Health supported this work.

REFERENCES

- Antonescu, C. N., G. Danuser, and S. L. Schmid. 2010. Phosphatidic acid plays a regulatory role in clathrin-mediated endocytosis. *Mol. Biol. Cell* **21**:2944–2952.
- Banno, Y. 2002. Regulation and possible role of mammalian phospholipase D in cellular functions. *J. Biochem.* **131**:301–306.
- Boucrot, E., S. Saffarian, R. Massol, T. Kirchhausen, and M. Ehrlich. 2006. Role of lipids and actin in the formation of clathrin-coated pits. *Exp. Cell Res.* **312**:4036–4048.
- Corrotte, M., et al. 2006. Dynamics and function of phospholipase D and phosphatidic acid during phagocytosis. *Traffic* **7**:365–377.
- Di Fulvio, M., K. Frondorf, K. M. Henkels, N. Lehman, and J. Gomez-Cambronero. 2007. The Grb2/PLD2 interaction is essential for lipase activity, intracellular localization and signaling in response to EGF. *J. Mol. Biol.* **367**:814–824.
- Di Fulvio, M., K. M. Henkels, and J. Gomez-Cambronero. 2007. Short-hairpin RNA-mediated stable silencing of Grb2 impairs cell growth and DNA synthesis. *Biochem. Biophys. Res. Commun.* **357**:737–742.
- Di Fulvio, M., N. Lehman, X. Lin, I. Lopez, and J. Gomez-Cambronero. 2006. The elucidation of novel SH2 binding sites on PLD2. *Oncogene* **25**:3032–3040.
- Frondorf, K., K. M. Henkels, M. A. Frohman, and J. Gomez-Cambronero. 2010. Phosphatidic acid (PA) is a leukocyte chemoattractant that acts through S6 kinase signaling. *J. Biol. Chem.* **285**:15837–15847.
- Higgs, H. N., and T. D. Pollard. 2000. Activation by Cdc42 and PIP(2) of Wiskott-Aldrich syndrome protein (WASP) stimulates actin nucleation by Arp2/3 complex. *J. Cell Biol.* **150**:1311–1320.
- Honda, A., et al. 1999. Phosphatidylinositol 4-phosphate 5-kinase alpha is a downstream effector of the small G protein ARF6 in membrane ruffle formation. *Cell* **99**:521–532.
- Huang, C. L. 2007. Complex roles of PIP2 in the regulation of ion channels and transporters. *Am. J. Physiol. Renal Physiol.* **293**:F1761–F1765.
- Insall, R. H., and L. M. Machesky. 2004. Regulation of WASP: PIP2 pipped by Toca-1? *Cell* **118**:140–141.
- Iyer, S. S., J. A. Barton, S. Bourgoin, and D. J. Kusner. 2004. Phospholipases D1 and D2 coordinately regulate macrophage phagocytosis. *J. Immunol.* **173**:2615–2623.
- Kim, A. S., L. T. Kakalis, N. Abdul-Manan, G. A. Liu, and M. K. Rosen. 2000. Autoinhibition and activation mechanisms of the Wiskott-Aldrich syndrome protein. *Nature* **404**:151–158.
- Knapek, K., et al. 2010. The molecular basis of phospholipase D2-induced chemotaxis: elucidation of differential pathways in macrophages and fibroblasts. *Mol. Cell. Biol.* **30**:4492–4506.
- Lehman, N., et al. 2006. Phagocyte cell migration is mediated by phospholipases PLD1 and PLD2. *Blood* **108**:3564–3572.
- Lehman, N., et al. 2007. Phospholipase D2-derived phosphatidic acid binds to and activates ribosomal p70 S6 kinase independently of mTOR. *FASEB J.* **21**:1075–1087.
- Lorenzi, R., P. M. Brickell, D. R. Katz, C. Kinnon, and A. J. Thrasher. 2000. Wiskott-Aldrich syndrome protein is necessary for efficient IgG-mediated phagocytosis. *Blood* **95**:2943–2946.
- Marchand, J. B., D. A. Kaiser, T. D. Pollard, and H. N. Higgs. 2001. Interaction of WASP/Scar proteins with actin and vertebrate Arp2/3 complex. *Nat. Cell Biol.* **3**:76–82.
- Miki, H., K. Miura, and T. Takenawa. 1996. N-WASP, a novel actin-depolymerizing protein, regulates the cortical cytoskeletal rearrangement in a PIP2-dependent manner downstream of tyrosine kinases. *EMBO J.* **15**:5326–5335.
- Miki, H., and T. Takenawa. 1998. Direct binding of the verprolin-homology domain in N-WASP to actin is essential for cytoskeletal reorganization. *Biochem. Biophys. Res. Commun.* **243**:73–78.
- Moritz, A., P. N. De Graan, W. H. Gispen, and K. W. Wirtz. 1992. Phosphatidic acid is a specific activator of phosphatidylinositol-4-phosphate kinase. *J. Biol. Chem.* **267**:7207–7210.
- Panchal, S. C., D. A. Kaiser, E. Torres, T. D. Pollard, and M. K. Rosen. 2003. A conserved amphipathic helix in WASP/Scar proteins is essential for activation of Arp2/3 complex. *Nat. Struct. Biol.* **10**:591–598.
- Papayannopoulos, V., et al. 2005. A polybasic motif allows N-WASP to act as a sensor of PIP2 density. *Mol. Cell* **17**:181–191.
- Park, H., and D. Cox. 2009. Cdc42 regulates Fc gamma receptor-mediated phagocytosis through the activation and phosphorylation of Wiskott-Aldrich syndrome protein (WASP) and neural-WASP. *Mol. Biol. Cell* **20**:4500–4508.
- Prehoda, K., J. A. Scott, R. D. Mullins, W. A. Lim. 2000. Integration of multiple signals through cooperative regulation of the N-WASP-Arp2/3 complex. *Science* **290**:801–806.
- Rohatgi, R., H. Y. Ho, and M. W. Kirschner. 2000. Mechanism of N-WASP

- activation by CDC42 and phosphatidylinositol 4,5-bisphosphate. *J. Cell Biol.* **150**:1299–1310.
28. **Scott, S. A., et al.** 2009. Design of isoform-selective phospholipase D inhibitors that modulate cancer cell invasiveness. *Nat. Chem. Biol.* **5**:108–117.
29. **Su, W., et al.** 2009. 5-Fluoro-2-indolyl des-chlorohalopemide (FIPI), a phospholipase D pharmacological inhibitor that alters cell spreading and inhibits chemotaxis. *Mol. Pharmacol.* **75**:437–446.
30. **Thrasher, A. J.** 2002. WASp in immune-system organization and function. *Nat. Rev. Immunol.* **2**:635–646.
31. **Thrasher, A. J., S. Burns, R. Lorenzi, and G. E. Jones.** 2000. The Wiskott-Aldrich syndrome: disordered actin dynamics in haematopoietic cells. *Immunol. Rev.* **178**:118–128.
32. **Tomasevic, N., et al.** 2007. Differential regulation of WASp and N-WASp by Cdc42, Rac1, Nck, and PI(4,5)P2. *Biochemistry* **46**:3494–3502.